Geomechanics and Engineering, *Vol. 39, No. 4 (2024) 369-383*
https://doi.org/10.12989/gae.2024.39.4.369

Effect of shield tunnel underpass construction on the upper existing pipeline

Zhen-Dong Cui*, Zhang-Lin Zhu, Xuan-Yu Mi, Li Yuan, Zhong-Liang Zhang and Chen-Yang Zhao

State Key Laboratory of Intelligent Construction and Healthy Operation & Maintenance of Deep Underground Engineering, School of Mechanics and Civil Engineering, China University of Mining and Technology, Xuzhou, Jiangsu, 221116, P.R. China

(*Received January 18, 2024, Revised October 17, 2024, Accepted November 11, 2024*)

Abstract. The construction of the shield tunnel results in the deformation of the surrounding soil and the existing pipeline. It is important to analyze the deformation of the existing pipeline during the excavation of the tunnel. Based on the two-stage analysis method, the shear effect of pipeline due to the uneven settlement was considered and the deformation and internal force of existing pipeline due to the tunnel excavation were studied. The theoretical formulas were verified by the in-site monitoring. Compared with the theoretical calculation, the three-dimensional numerical simulation was established to simulate the deformation of the existing pipeline and the ground surface during the tunnelling. The effect of the Poisson's ratio, the tunnel diameter and the pipeline shading on the deformation of the existing pipeline were further investigated. The results show that the deformation curves of the pipeline and the ground surface conform to the Gaussian distribution, and the position above the axis of the tunnel experiences the maximum. When the excavation surface of tunnel crosses underneath the pipeline, the pipeline and the ground surface experience larger deformation and more subsidence, respectively. A certain amount of uplift is generated for the pipeline and the ground surface at ± 20 m away from the center line of the tunnel. The deformation of existing pipelines is affected by the tunnel excavation within its diameter range. The results can provide a reference for the design and construction of the shield tunnel underpass.

Keywords: existing pipeline; shield tunnel; shielding effect of pipeline; underpass construction; vertical deformation of pipeline

1. Introduction

The construction of urban subway tunnel causes the deformation of the surrounding soil, resulting in the deformation of the buried pipeline. Therefore, the safety of the underground pipeline has been concerned. At present, there are three main research methods for the deformation of existing pipelines caused by tunnel excavation, including the theoretical analysis method (Attewell *et al.* 1986, Klar *et al.* 2005, Liu *et al.* 2022), the numerical simulation (Klar *et al.* 2007, Lin *et al.* 2019), and the model test (Vorster *et al.* 2006, Marshall *et al.* 2010, Zhang *et al.* 2023). Attewell *et al.* (1986) first simulated the impact of tunnel construction on underground pipelines based on the Winkler model of elastic foundation beams to obtain the analytical solutions for the pipelines in the parallel or vertical of the tunnel. The existing pipelines were simplified to be the Euler Bernoulli beam by Liang *et al.* (2016) and Lin *et al.* (2020) and the Timoshenko beam by Liang *et al.* (2017) and Liu *et al.* (2020), respectively. The interactions between pipelines and soils were taken as the Winkler foundation model (Huang *et al.* 2019), the elastic-continuum model (Klar *et al.* 2005, Klar *et al.* 2008), the Pasternak foundation model (Liang *et al.* 2018), and the Vlasov foundation model (Wu *et al.* 2018), respectively. The impact of the tunnel undercrossing to the existing pipeline were studied by the two-stage analysis method, including the burial depth of pipeline, the stiffness of pipeline (Zhang *et al.* 2015) and relative position of pipeline and tunnel (Huang *et al.* 2019). The deformations of the soil and the existing pipeline resulting from the tunnel excavation were studied and the modified stochastic medium method and the Winkler foundation beam were conducted (Zhang *et al.* 2016). The soil-pipeline interaction of the tunnel orthogonally passing under two existing pipelines were studied by Lin *et al.* (2021). The elastic-continuum model and the Pasternak model were conducted to calculate the deflections and bending moment of the two neighboring pipelines above the tunnel, and the effects of the horizontal distance, bending stiffness and burial depth on the deflections and bending moment were investigated. Ding *et al.* (2023) calculated the deformation of the existing tunnel caused by the excavation of the large-diameter slurry shield based on two-stage method and found that the crossing angle on maximum settlement and the influence range of settlement of the existing tunnel had a significant influence.

The numerical simulation has the advantages of repeatable computation, efficiency, economy, and operability which is widely used in the tunnel construction. The stress and deformation of the polyethylene (PE) pipeline under the surface settlement were simulated by Luo *et al.* (2015), considering the mutual perpendicularity between the PE pipeline and the section experiencing the settlement. Huang *et al.* (2013) studied the deformation of existing pipeline caused by nearby deep foundation pit excavation, considering the relative position between the tunnel and the pipeline, the tunnel diameter, and the

*Corresponding author, Ph.D.
E-mail: cuizhendong@cumt.edu.cn

http://www.techno-press.org/?journal=gae&subpage=7
ISSN: 2005-307X (Print), 2092-6219 (Online)

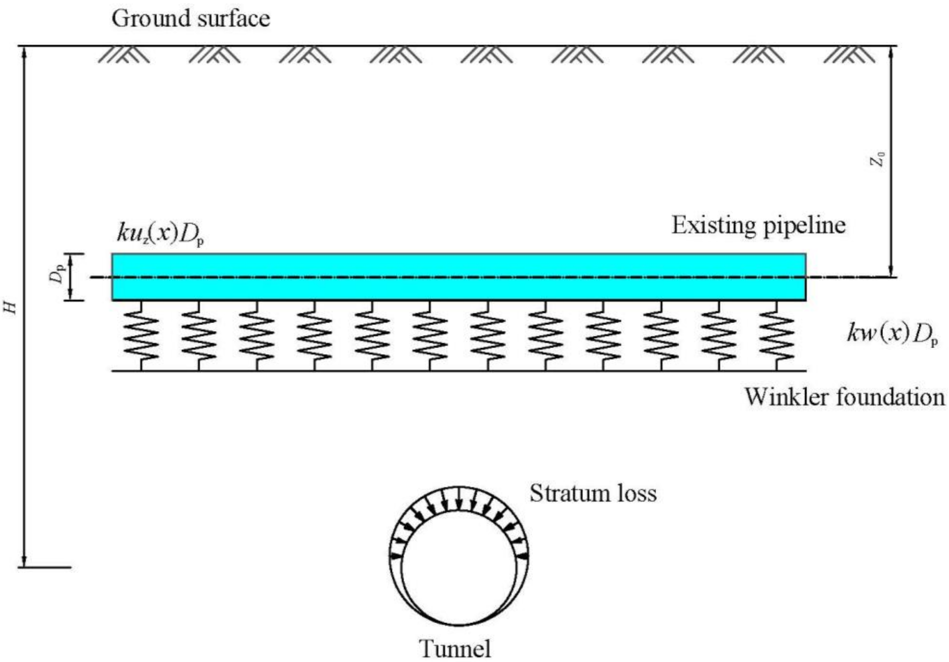

Fig. 1 The model diagram

protection measures for tunnel. Through the finite element analysis, the position of the pipeline crossed vertically by the tunnel was not the most dangerous, so the deformation and stress of existing pipeline were underestimated (Wang *et al.* 2011, Shi *et al.* 2013). A parametric study on the effect of tunnel construction on the lining member forces and stresses of the existing tunnel was simulated by Yoo and Cui (2020). Considering the tunnel size, the buried depth of tunnel, the relative position between two tunnels and the lining thickness, the interaction resulting from the simultaneous excavation of the parallel tunnels was studied (Nawel and Salah 2015). Chen *et al.* (2023) studied the effect of the existing tunnel in operation due to the excavation of the horizontal offset of the divergence tunnel. Lin *et al.* (2019) studied the effect of tunnel angle on the deformation of the existing tunnels and the ground surface and found the deformation and internal force of the existing tunnel and the surface deformation appeared asymmetric characteristics obviously. Chen *et al.* (2022) explored the effect of different tunnel shapes on the complicated tunnel-tunnel interaction and found that the volume loss played the most important role in the multi-tunnel interactions. Shi *et al.* (2022) studied the deformation of the discontinuous pipelines due to the tunnel excavation and found that the deformation of the pipelines increased with the buried depth of the pipelines increasing and the buried depth of the tunnel decreasing. The impacts of the horizontal distance of pipelines, the diameter of pipeline, the thickness of pipeline, and the method of excavation on the response of the neighboring underground pipeline were simulated through FLAC3D (Wang *et al.* 2022). Zhang *et al*. (2024) studied the excavation of the small radius curve shield tunnel and found that the peak of stratum horizontal deformation appeared near the axis of tunnel.

The commonly used theoretical analysis methods mainly considered that the longitudinal deformation of pipelines was mainly caused by the bending deformation, while the impact of pipeline shear deformation on the longitudinal deformation of the pipeline was normally ignored. In addition, the influencing factors of pipeline deformation mainly focused on the spacing between pipe and tunnel, the stiffness of pipeline, and the burial depth of pipeline. However, the soil parameters around the pipeline and the diameter of tunnel were less studied. In this paper, the impact of tunnel underpass construction on the deformation of existing pipeline were studied by the Timoshenko beam theory considering the influence of shear deformation on pipeline deformation. Considering the shielding effect of pipeline was considered to study the deformation effect of tunnel excavation on the existing pipeline and its overlying soil a under different soil Poisson's ratios and tunnel diameters were studied through the numerical simulation.

2. Theoretical analyses

2.1 Model assumptions

The construction process of tunnel results in the loss of stratum, the displacement of surrounding soil, and the additional internal forces and displacements for the existing pipeline. Fig. 1 illustrates the theoretical model for the impact of tunnel construction on the existing pipeline. In order to simplify the theoretical calculation, the following assumptions are as follows.

(1) The existing pipeline is considered as the Timoshenko beam with the shear effect;

(2) Both ends of the beams are located outside the influence of the tunnel excavation;

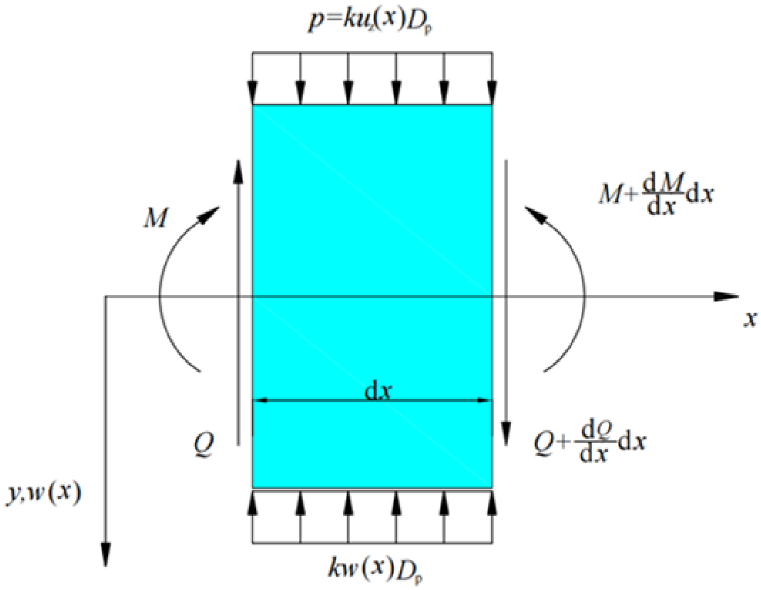

Fig. 2 Theoretical analysis of model

(3) The interaction between the existing pipeline and the ground is considered through the Winkler foundation model, and the contact is always maintained over the interface of the pipeline and the surrounding soils;

(4) The original deformation of the existing pipeline is neglected and the time effects of the interaction between the strata and the pipeline is not considered, such as the creep and the consolidation.

The calculation model is based on the derivation of a two-stage analysis. In the first step, the free displacement of the surrounding soil caused by the construction of the new tunnel is analyzed without considering the presence of the existing pipeline. In the second step, the free displacement of soil body acts on the existing pipeline as a displacement load, so the equilibrium differential equations of the coupling of the soil body displacement and pipeline structure deformation, and the finite difference method is conducted to derive the theoretical solution of the pipeline displacement due to the tunnel excavation.

2.2 Soil displacement due to the excavation of tunnel

The theoretical solution of Loganathan and Poulos method (Loganathan and Poulos 1998) was utilized to predict the surrounding soil displacement caused by the construction of tunnel. The vertical displacement is shown in Eq. (1).

$$u_z(x) = -R^2 x\left[\frac{1}{x^2+(H-z)^2}+\frac{3-4\nu}{x^2+(z+H)^2}-\frac{4z(z+H)}{\left[x^2+(z+H)^2\right]^2}\right] \cdot\frac{4gR+g^2}{4R^2}\exp\left\{-\left[\frac{1.38x^2}{(H+R)^2}+\frac{0.69z^2}{H^2}\right]\right\} \tag{1}$$

where $u_z(x)$ is the vertical displacement of the ground surface; R is the radius of the tunnel excavation; H is the distance from the tunnel axis to the ground surface; g is the clearance coefficient (Lee *et al.* 1992); ν is the Poisson's ratio; x is the horizontal distance from the tunnel axis; and z is the vertical distance of the soil layer from the tunnel axis.

2.3 Longitudinal deformation analysis of the existing pipeline

From Fig. 2, the equations for the force and the bending moment are obtained by specifying the pipe settlement as positive direction shown in Eqs. 2(a) and 2(b), respectively.

$$Q + kw(x)D_{\mathrm{p}}\mathrm{d}x = Q + \frac{\mathrm{d}Q}{\mathrm{d}x}\mathrm{d}x + ku_z(x)D_{\mathrm{p}}\mathrm{d}x \tag{2a}$$

$$M + Q\mathrm{d}x + kw(x)D_{\mathrm{p}}\frac{\mathrm{d}x^2}{2} = M + \frac{\mathrm{d}M}{\mathrm{d}x}\mathrm{d}x + ku_z(x)D_{\mathrm{p}}\frac{\mathrm{d}x^2}{2} \tag{2b}$$

where k is the coefficient of foundation; D_{p} is the diameter of the existing pipeline; $w(x)$ is the vertical displacement; Q is the shear force; and M is the bending moment.

Based on Timoshenko's beam theory (Timoshenko 1921, 1922), the relationship between M and θ is shown in Eq. 3(a). The Q, the $w(x)$ and the θ are shown in Eq. 3(b).

$$M = -EI\frac{\mathrm{d}\theta}{\mathrm{d}x} \tag{3a}$$

$$Q = GA\left[\frac{\mathrm{d}w(x)}{\mathrm{d}x} - \theta\right] \tag{3b}$$

where E and G are the Young's modulus and shear modulus, respectively; I is the section moment of inertia; and A is the section area.

Substituting Eqs. 3(a) and 3(b) into Eqs. 2(a) and 2(b), and omitting the higher-order micrometric quantities, the equilibrium differential equation for the vertical displacement $w(x)$ of the existing pipeline under the displacement load is obtained.

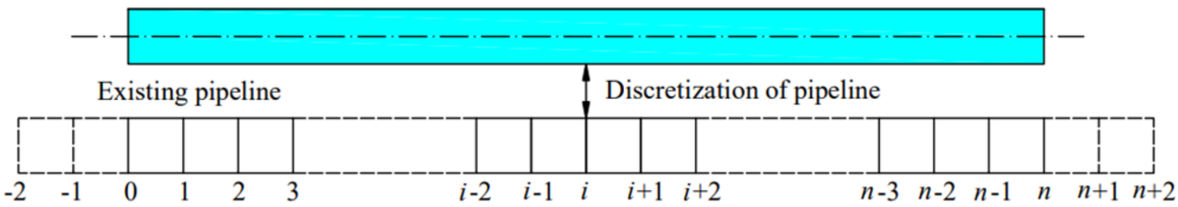

Fig. 3 Pipeline discretization

$$\frac{d^4 w(x)}{dx^4} - \frac{kD_p}{GA}\frac{d^2 w(x)}{dx^2} + \frac{kD_p}{EI} w(x) = \frac{kD_p}{EI} u_z(x) - \frac{kD_p}{GA}\frac{d^2 u_z(x)}{dx^2} \quad (4)$$

The effect of tunnel excavation on the longitudinal deformation of the existing pipeline is obtained by the finite difference method. The discretization for the pipeline is shown in Fig. 3 and the finite difference form of Eq. (4) is shown in Eq. (5).

$$\frac{6w_i - 4(w_{i+1} + w_{i-1}) + (w_{i+2} + w_{i-2})}{l^4} - \frac{kD_p}{GA}\frac{w_{i+1} - 2w_i + w_{i-1}}{l^2} + \frac{kD_p}{EI} w_i = \frac{kD_p}{EI} u_{z,i} - \frac{kD_p}{GA}\frac{u_{z,i+1} - 2u_{z,i} + u_{z,i-1}}{l^2} \quad (5)$$

where $u_{z,i}$, $u_{z,i+1}$ and $u_{z,i-1}$ are the vertical displacements of the soil caused by the tunnel excavation at node units i, $i+1$ and $i-1$, respectively.

According to Eqs. 3(a) and 3(b), the equilibrium differential equations for the longitudinal distribution of shear force Q and bending moment M of the existing pipeline under the displacement loading are shown in Eqs. 6(a) and 6(b), respectively.

$$Q = -EI\left[\frac{d^3 w(x)}{dx^3} - \frac{kD_p}{GA}\frac{dw(x)}{dx} + \frac{kD_p}{GA}\frac{du_z(x)}{dx}\right] \quad (6a)$$

$$M = -EI\left[\frac{d^2 w(x)}{dx^2} - \frac{kD_p}{GA} w(x) + \frac{kD_p}{GA} u_z(x)\right] \quad (6b)$$

The finite difference forms of Eqs. 6(a) and 6(b) are obtained, shown in Eqs. 7(a) and 7(b), respectively.

$$Q_i = -EI\left(\frac{w_{i+2} - 2w_{i+1} + 2w_{i-1} - w_{i-2}}{2l^3} - \frac{kD_p}{GA}\frac{w_{i+1} - w_{i-1}}{2l} + \frac{kD_p}{GA}\frac{u_{z,i+1} - u_{z,i-1}}{2l}\right) \quad (7a)$$

$$M_i = -EI\left(\frac{w_{i+1} - 2w_i + w_{i-1}}{l^2} - \frac{kD_p}{GA} w_i + \frac{kD_p}{GA} u_{z,i}\right) \quad (7b)$$

Assuming that both ends of the pipe are free, the shear force Q and bending moment M are zero at both ends of the pipeline.

$$Q_0 = Q_n = 0 \quad (8a)$$

$$M_0 = M_n = 0 \quad (8b)$$

Combined with Eqs. 8(a) and 8(b), the finite difference equations for the bending moment M and shear force Q at both ends of the pipeline are obtained when node i is equal to 0 or n, shown in Eqs. 9(a)- 9(d).

$$Q_0 = -EI\left(\frac{w_2 - 2w_1 + 2w_{-1} - w_{-2}}{2l^3} - \frac{kD_p}{GA}\frac{w_1 - w_{-1}}{2l} + \frac{kD_p}{GA}\frac{u_{z,1} - u_{z,-1}}{2l}\right) \quad (9a)$$

$$Q_n = -EI\left(\frac{w_{n+2} - 2w_{n+1} + 2w_{n-1} - w_{n-2}}{2l^3} - \frac{kD_p}{GA}\frac{w_{n+1} - w_{n-1}}{2l} + \frac{kD_p}{GA}\frac{u_{z,n+1} - u_{z,n-1}}{2l}\right) \quad (9b)$$

$$M_0 = -EI\left(\frac{w_1 - 2w_0 + w_{-1}}{l^2} - \frac{kD_p}{GA} w_0 + \frac{kD_p}{GA} u_{z,0}\right) \quad (9c)$$

$$M_n = -EI\left(\frac{w_{n+1} - 2w_n + w_{n-1}}{l^2} - \frac{kD_p}{GA} w_n + \frac{kD_p}{GA} u_{z,n}\right) \quad (9d)$$

To solve this pair of simultaneous equations, the deflection of the extra virtual nodes at the two ends of the tunnel are obtained, shown in Eqs. 10(a)-10(d).

$$w_{-1} = \left(\frac{kD_p l^2}{GA} + 2\right) w_0 - w_1 - \frac{kD_p l^2}{GA} u_{z,0} \quad (10a)$$

$$w_{-2} = \left(\frac{k^2 D_p^2 l^4}{G^2 A^2} + \frac{4kD_p l^2}{GA} + 4\right) w_0 - \left(\frac{2kD_p l^2}{GA} + 4\right) w_1 + w_2 - \left(\frac{k^2 D_p^2 l^4}{G^2 A^2} + \frac{2kD_p l^2}{GA}\right) u_{z,0} + \frac{kD_p l^2}{GA}\left(u_{z,1} - u_{z,-1}\right) \quad (10b)$$

$$w_{n+1} = \left(\frac{kD_p l^2}{GA} + 2\right) w_n - w_{n-1} - \frac{kD_p l^2}{GA} u_{z,n} \quad (10c)$$

$$w_{n-2} = \left(\frac{k^2 D_p^2 l^4}{G^2 A^2} + \frac{4kD_p l^2}{GA} + 4\right) w_n - \left(\frac{2kD_p l^2}{GA} + 4\right) w_{n+1} + w_{n+2} - \left(\frac{k^2 D_p^2 l^4}{G^2 A^2} + \frac{2kD_p l^2}{GA}\right) u_{z,n} + \frac{kD_p l^2}{GA}\left(u_{z,n+1} - u_{z,n-1}\right) \quad (10d)$$

The matrix form of Eq. (5) is shown in Eq. (11).

$$\left([K_1] - [K_2] + [K_3]\right)\{w\} = \{U_1\} - \{U_2\} \quad (11)$$

where $[K_1]$ is the displacement stiffness matrix of pipeline; $[K_2]$ is the shear stiffness matrix of pipeline; $[K_3]$ is the flexural stiffness matrix of pipeline; $\{w\}$ is the vertical displacement matrix of pipeline; $\{U_1\}$ is the vertical displacement matrix of soil caused by the construction of tunnel; and $\{U_2\}$ is the vertical displacement correction

Table 1 Parameters of theoretical calculation (Wu 2008)

Parameters	R (m)	H (m)	z_0 (m)	g	E_s (MPa)	ν	E (GPa)
Value	3.0	14.4	8.7	0.03	8.2	0.3	52

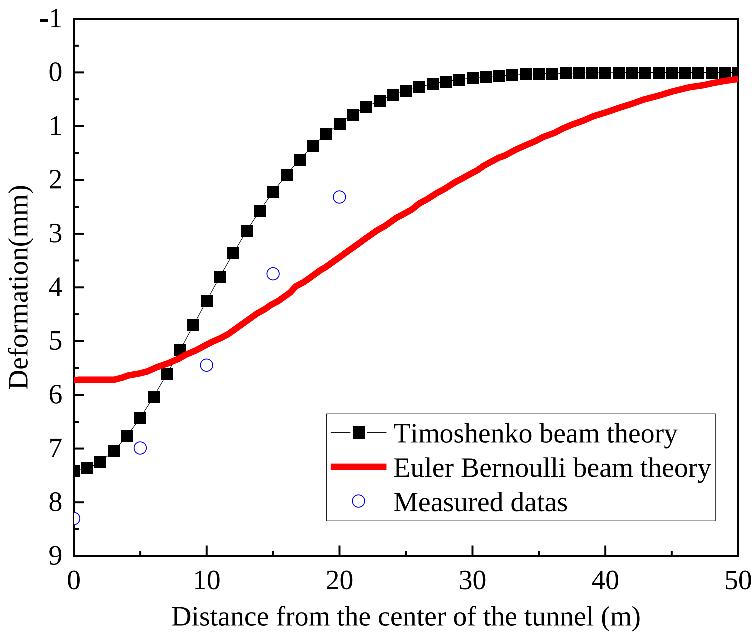

Fig. 4 Variations of deformation with distance from the center of the tunnel

matrix of soil caused by the construction of tunnel. The full expressions of $[K_1]$, $[K_2]$, $[K_3]$, $\{U_1\}$ and $\{U_2\}$ are presented in Appendix A.

Let $[K] = [K_1] - [K_2] + [K_3]$, $\{U\} = \{U_1\} - \{U_2\}$, and multiply both sides of Eq. (11) by $[K]^{-1}$, then the vertical displacement matrix $\{w\}$ of pipeline is obtained, shown in Eq. (12).

$$\{w\} = [K]^{-1}\{U\} \tag{12}$$

where $[K]^{-1}$ is the inverse matrix of matrix $[K]$.

With the known soil displacement $u_z(x)$, the theoretical solution for the vertical displacement $\{w\}$ of the existing pipeline is obtained from Eq. (12). Substituting the obtained $\{w\}$ into Eqs. 7(a) and 7(b), the shear force Q and bending moment M of the existing pipeline under the construction of the tunnel is obtained.

2.4 Model verification

In order to verify the theoretical formulas, the displacement monitoring data of the existing pipeline were obtained based on the background of the deformation of the existing pipeline above the tunnel caused by the construction of the section between Yitian Station and Xiangmihu Station in Shenzhen Metro Phase 1 project (Wu 2008). In addition, the calculation results are compared with those by Euler Bernoulli beam theory. The shield tunneling vertically underpasses the concrete pipeline, 3.0 m in diameter, 0.12 m in thickness, and 8.7 m in buried depth along the central axis of the pipeline. The specific parameters are summarized in Table 1.

Fig. 4 illustrates the variations of the longitudinal deformation of the pipeline with the distance from the centerline of the tunnel. The section of pipeline at the centerline of the tunnel experiences the maximum deformation, 5.73 mm by Euler Bernoulli beam method and 7.41 mm by Timoshenko beam method and their errors are 31.0% and 10.8% comparing with 8.31 mm by in-site monitoring, respectively. The inflection point of the deformation curve for the theoretical solution of Timoshenko beam method is approximately 20 m away from the centerline of the tunnel, while it is 30 m for Euler Bernoulli beam method. The deformation of the pipeline is 0 at about 30 m and 50 m away from the centerline of the tunnel by Timoshenko beam method and Euler Bernoulli beam method, respectively. The longitudinal deformation of the pipeline and its trend by Timoshenko beam method are closer to the results of in-site monitoring than those by Euler Bernoulli beam method. The feasibility and accuracy of the theoretical calculation are proved.

3. Numerical simulations

3.1 Assumptions and dimensions of models

The construction of the shield tunnel results in the loss of stratum, the deformation of the surrounding soil and the existing pipeline. The deformation of the soil and the pipeline are affected with the geological and construction conditions and the parameters of the shield. Therefore, the model is based on the following assumptions.

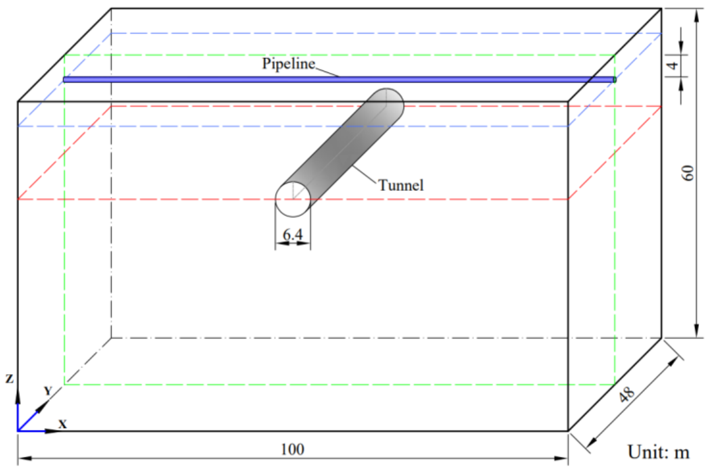

Fig. 5 Position of the tunnel and existing pipeline and model size

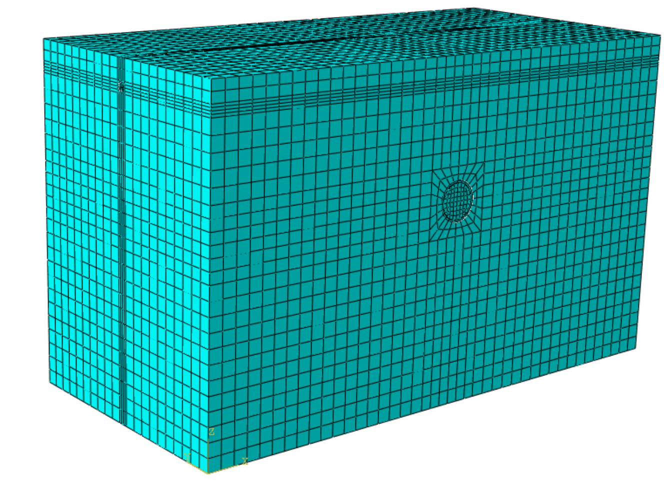

(a) Model meshing

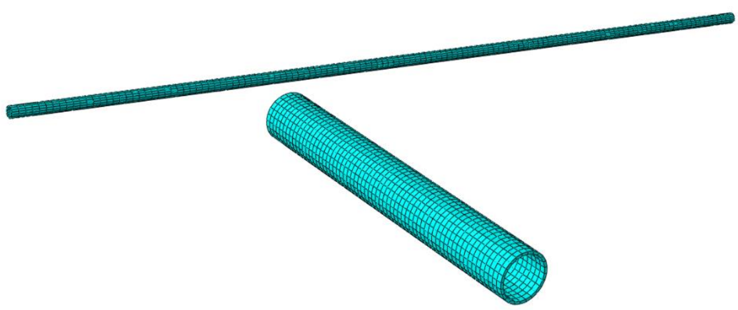

(b) Pipeline, lining and grouting layer meshing

Fig. 6 Numerical simulation model

(1) The isotropic sandy soil is considered;

(2) The groundwater, the pore pressure, the fluid-structure interaction and the creep are neglected;

(3) The plastic deformation of the pipeline, the lining and the grouting layer are not considered.

Fig. 5 illustrates the relative positions of the tunnel and existing pipeline in the soil. A comprehensive model was established using ABAQUS, consisting of the shield tunnel, the pipeline and the sandy soil field as illustrated in Fig. 6. The width of the sandy soil site in the numerical model was 100 m,

Table 2 Characteristics of the model

Parts	Material properties	γ (kN/m^3)	E (MPa)	μ	φ
Soil field	Mohr-Coulomb elastic-plasticity	17.5	40	0.25	35°
Pipeline	linear elasticity	20.0	15	0.20	-
Lining Grouting layer	linear elasticity	25.0	25×10^3	0.20	-

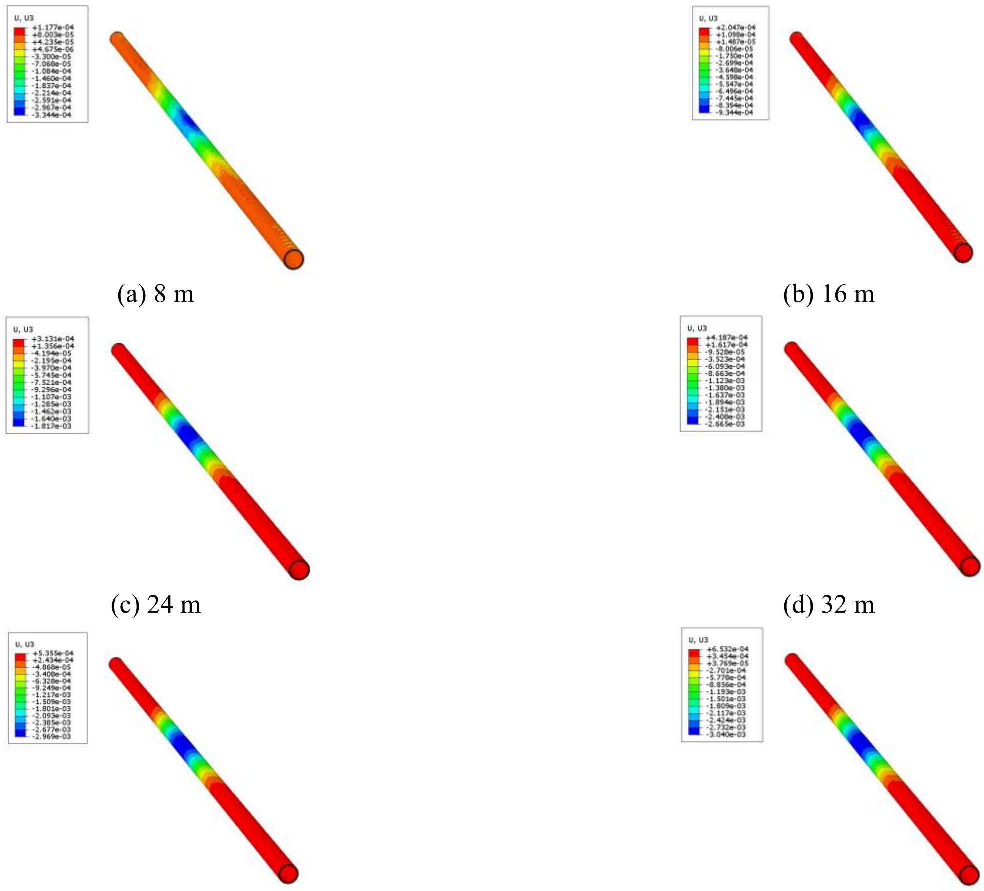

(a) 8 m (b) 16 m

(c) 24 m (d) 32 m

(e) 40 m (f) 48 m

Fig. 7 Longitudinal deformation nephograms of pipeline with different tunnel excavation distances

which is more than five times the diameter of the shield tunnel. Thus, the influence of boundary conditions on the deformation of the pipeline was eliminated. The diameters of the shield tunnel and the pipeline are 6.4 m and 1.0 m, respectively. The burial depth of the pipeline is 4 m. The clearance between the pipeline and the tunnel is two time of the diameter of the tunnel. The thickness of the lining, the equivalent layer and the pipeline is 0.35 m, 0.10 m, and 0.12 m, respectively. The grouting pressure is 200 kPa. The parameters of material of model are summarized in Table 2. The soil is excavated by shield tunneling according to the ring. The length of the ring is 2 m. The C3D8 element is used for the model. The radial of pipeline and the tunnel and the depth of soil are the direction of X, Y and Z, respectively.

3.2 Excavation process

The method of the life and death element is used in the numerical simulation. The specific steps are as follows.

(1) The elements of the grouting layer, the shield and the lining are "killed". The geo-stress is balanced;

(2) The first ring of the soil is excavated: this element of the soil is "killed" and the pressure of the tunnel face and grouting are activated;

(3) The following ring of soil is excavated and the elements of the grouting layer and the lining for the previous ring are activated;

(4) Repeat step (3) until the excavation is over.

3.3 Numerical results

Fig. 7 illustrates the nephogram of the variations of the deformation of pipeline under different depths of excavation. The deformation of pipeline gradually increases with the depth of excavation increasing. The longitudinal deformation of pipeline at the radial middle position is maximum, decreasing

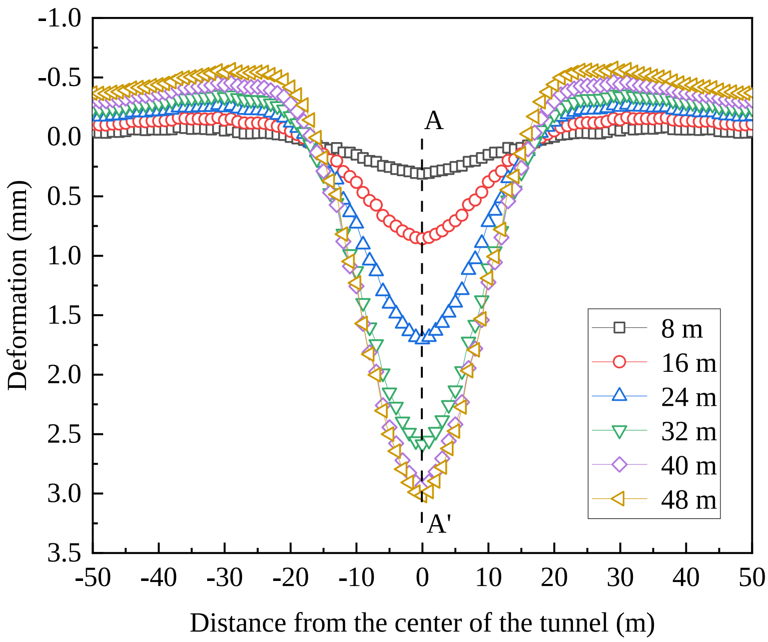

(a) Existing pipeline

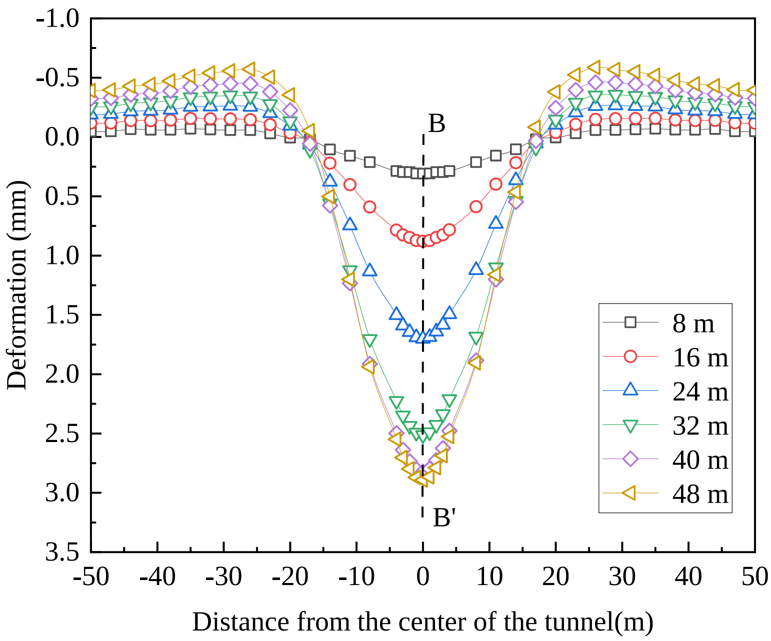

(b) Surface soil above the pipeline

Fig. 8 Variations of deformation with distance from the center of the tunnel under different distances of tunnel excavation

towards both sides gradually. On both sides of the pipeline experiences a slight uplift.

The variations of longitudinal deformation of the pipeline and the surface soil above pipeline with the distance from the centerline of the tunnel under different depths of excavation are illustrated in Fig. 8. It is shown in Fig. 8(a) that the longitudinal deformation curve of pipeline conforms to the settlement trough and Gaussian curve. When the depth of excavation is 16 m, the pipeline appears a slightly uplift at approximately 20 m away from the centerline of the tunnel. The uplift increases gradually with excavating. When the tunnel face completely underpasses the pipeline, the increase of pipeline experiences the maximum. Fig. 9 illustrates the variations of maximum deformation of existing pipeline with different distances of tunnel excavation. With the depth of excavation of 8 m, 16 m, 24 m, 32 m, 40 m and 48 m, the maximum longitudinal deformation of pipeline is 0.31 mm, 0.86 mm, 1.70 mm, 2.58 mm, 2.93 mm and 3.02 mm, the increase is 0.55 mm, 0.84 mm, 0.88 mm, 0.35 mm and 0.09 mm, respectively. Before the tunnel face underpassing the pipeline, the increase of pipeline increases with the tunnel face close to the section of pipeline, while the increase of pipeline decreases with the tunnel face

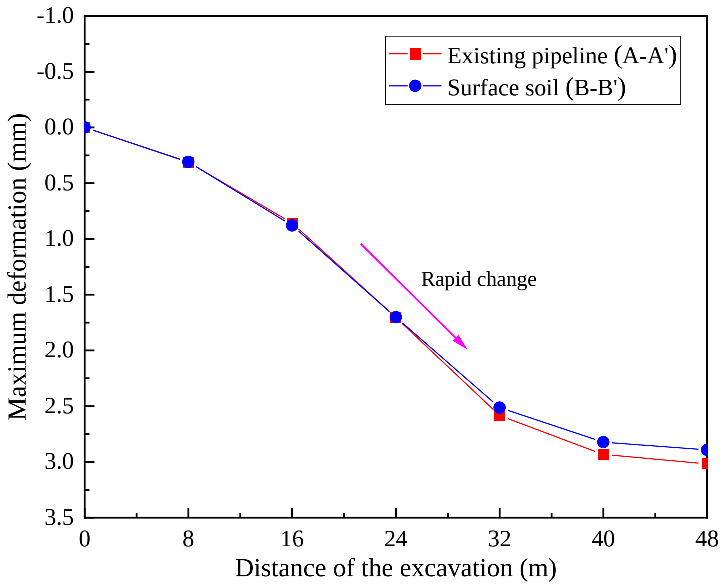

Fig. 9 Variations of maximum deformation of existing pipeline and surface soil with different distances of tunnel excavation

away from the pipeline after the tunnel face underpassing the pipeline. The pipeline experiences a significant settlement when the tunnel underpasses the pipeline, which can be an important stage resulting in the pipeline damaged.

Fig. 8(b) illustrates the variations of the longitudinal deformation of surface soil above pipeline with the distance from the centerline of the tunnel under different depths of excavation. The surface soil above the centerline of the tunnel experiences the maximum deformation. The deformation decreases towards both sides gradually. The longitudinal deformation curve of surface soil conforms to the settlement trough and Gaussian curve. The deformation of surface soil increases gradually with the depth of excavation increasing. Fig. 9 illustrates the variations of maximum deformation of surface soil with different distances of tunnel excavation. With the depth of excavation of 8 m, 16 m, 24 m, 32 m, 40 m and 48 m, the maximum longitudinal deformation is 0.30 mm, 0.86 mm, 1.70 mm, 2.51 mm, 2.82 mm and 2.89 mm and the increase is 0.56 mm, 0.84 mm, 0.81 mm, 0.31 mm and 0.07 mm, respectively. With the depth of excavation is 16 m, the surface soil appears an uplift at approximately 20 m away from the centerline of the tunnel. The uplift increases gradually with excavating. The longitudinal deformation of surface soil above pipeline is consistent with those of pipeline resulting from the continuity of soil.

4. Parametric studies

In the following, parametric studies, in terms of the soil Poisson's ratio, the diameter of tunnel and the shielding effect of pipeline, are considered in the model.

4.1 Influence of Poisson's ratio

Fig. 10 illustrates the variations of the longitudinal deformation of the pipeline and the surface soil above pipeline with the distance from the centerline of the tunnel under different Poisson's ratios. As shown in Fig. 10(a), the maximum deformation of pipeline is located above the centerline of the tunnel, and decreases with the Poisson's ratio increasing. When the Poisson's ratio increases from 0.2 to 0.35, the maximum deformation of pipeline decreases from 3.02 mm to 2.62 mm, accounting for 13.2%. The deformation of the surrounding soil is induced by the tunnel excavation, which results in the deformation of pipeline. With the Poisson's ratio increasing, the deformation of soil and pipeline decrease. The width of settlement trough is approximately 30 m under different Poisson's ratios. The pipeline experiences an uplift at above 15 m away from the centerline of the tunnel. The deformation of pipeline is 75% of the maximum at approximately 7 m away from the centerline of the tunnel. The main deformation zone of pipeline affected by the tunnel excavation is within 7 m at both sides of tunnel, which should not be influenced by the Poisson's ratio.

From Fig. 10(b), the maximum deformation of surface soil is located above the centerline of the tunnel, which decreases with the Poisson's ratio increasing. The deformation curve of surface soil conforms to the settlement trough, and the width of the settlement trough is approximately 26 m under different Poisson's ratios. The pipeline experiences an uplift at above 13 m away from the centerline of the tunnel. The longitudinal deformation of surface soil above pipeline is consistent with those of pipeline resulting from the continuity of soil.

Fig. 11 illustrates the variations of the longitudinal deformation of the pipeline with the distance from the centerline of the tunnel at the Poisson's ratio of 0.2. The deformation law of pipeline by numerical stimulation is basically consistent to the theoretical calculation. The section of pipeline at the centerline of the tunnel experiences the maximum deformation and the longitudinal deformation curve of pipeline conforms to the settlement trough by numerical stimulation and theoretical calculation. The width of the settlement trough is approximately 60 m and 30 m for the theoretical calculation and numerical stimulation, respectively.

The pipeline experiences a slightly uplift at above 15 m

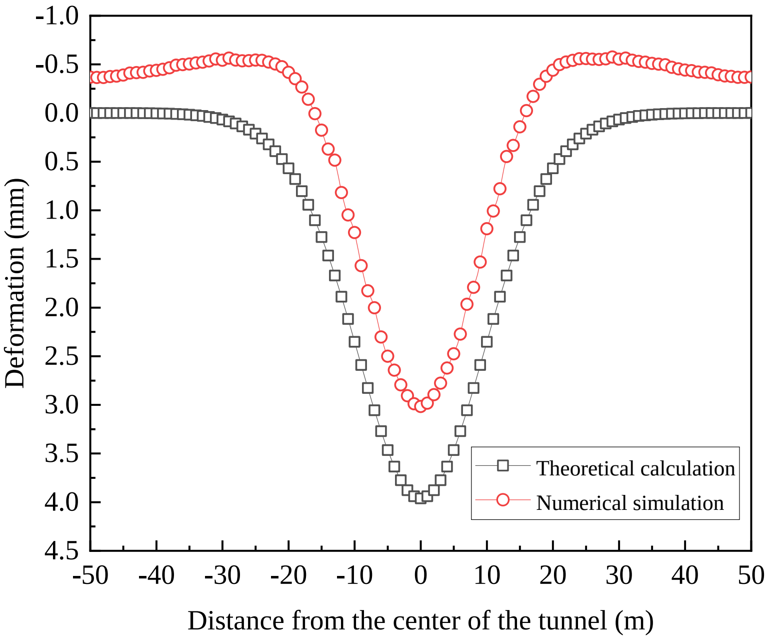

(a) Existing pipeline

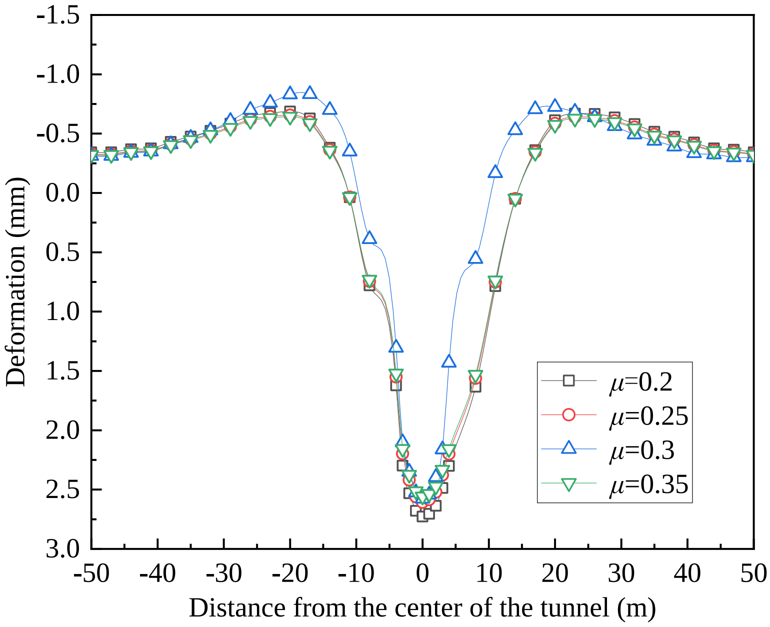

(b) Surface soil above the pipeline

Fig. 10 Variations of deformation with distance from the center of the tunnel under different Poisson's ratios

away from the centerline of the tunnel by the numerical stimulation, while it only has settlement by the theoretical calculation. For the lining and the grouting pressure being considered, the longitudinal deformation of pipeline of the numerical stimulation is smaller than those of the theoretical calculation.

4.2 Influence of the tunnel diameter

Fig. 12 illustrates the variations of the longitudinal deformation of the pipeline and the surface soil above pipeline with the distance from the centerline of the tunnel under the different diameters of tunnel. From Fig. 12(a), the maximum deformation of pipeline is located above the centerline of the tunnel, which increases with the diameter of tunnel increasing. With the diameter of tunnel increasing from 4 m to 10 m, the maximum deformation of pipeline increases from 2.80 mm to 22.77 mm. The deformation curve of the pipeline is changed from the type of "U" to "V". Especially, the maximum deformation of the pipeline increases significantly with the tunnel diameter increasing from 6.4 m to 8 m and from 8 m to 10 m, respectively. The deformation curve of surface soil conforms to the settlement trough. The deformation of the pipeline is 0 at about 20 m and 25 m away from the centerline of the tunnel when the diameter of tunnel is 4 m, 6.4 m and 8

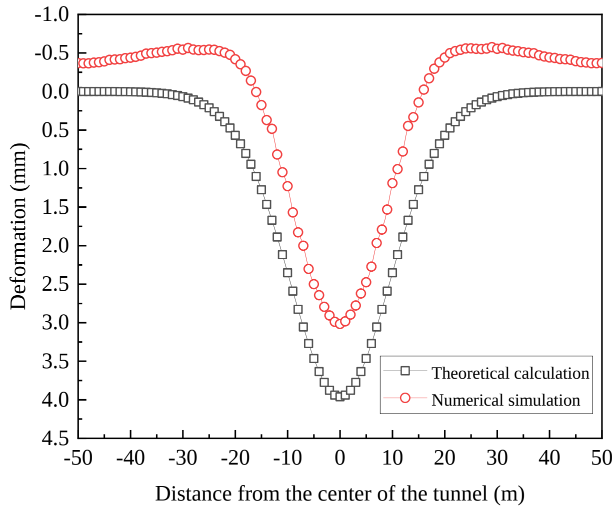

Fig. 11 Variations of deformation with distance from the center of the tunnel under theoretical calculation and numerical simulation (μ = 0.2)

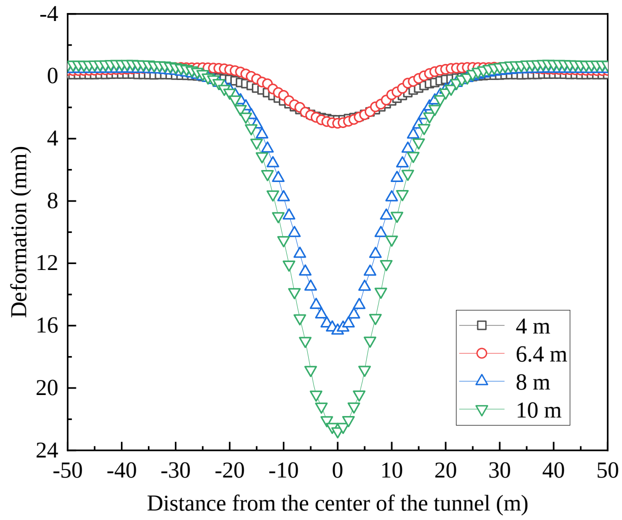

(a) Existing pipeline

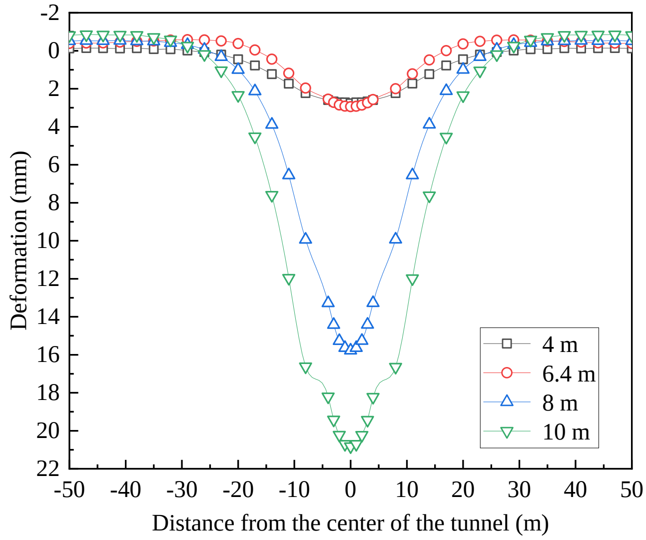

(b) Surface soil above the pipeline

Fig. 12 Variations of deformation with distance from the center of the tunnel under different diameters of tunnel

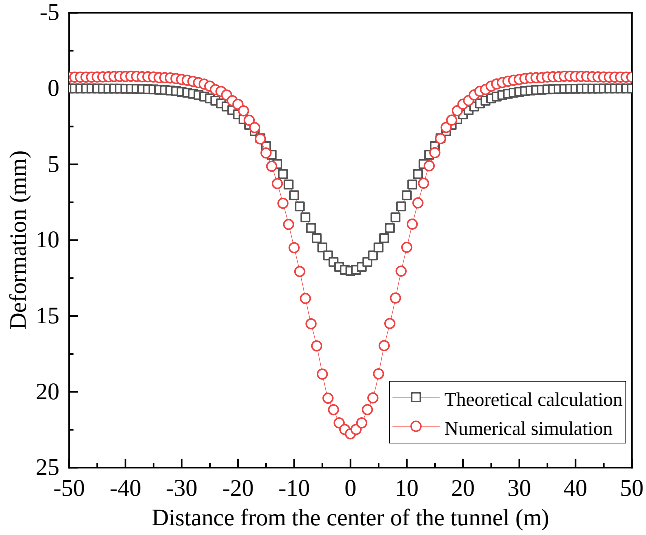

Fig. 13 Variations of deformation with distance from the center of the tunnel under theoretical calculation and numerical simulation (D = 10 m)

m, 10 m, respectively. The deformation of pipeline is 75% of the maximum at about 7 m away from the centerline of the tunnel. The main deformation zone of pipeline affected by the tunnel excavation is within 7 m at both sides of tunnel, which is not influenced by the changing of the tunnel diameter. It is indicated that the tunnel diameter has great effects on the longitudinal deformation of the pipeline.

From Fig. 12(b), the maximum deformation of surface soil is located above the centerline of the tunnel. The deformation curve of surface soil conforms to the settlement trough, and decreases towards both sides gradually. The width of the surface settlement trough is about 40 m for the tunnel diameter being 4 m and 6.4 m, while it is about 50 m for the tunnel diameter being 8 m and 10 m. The longitudinal deformation of surface soil above pipeline is consistent with that of pipeline resulting from the continuity of soil.

Fig. 13 illustrates the variations of the longitudinal deformation of the pipeline with the distance from the centerline of the tunnel when the diameter of tunnel is 10 m.

The deformation law of pipeline by numerical stimulation is basically consistent to the theoretical calculation. The section of pipeline at the centerline of the tunnel both experiences the maximum deformation and the longitudinal deformation curve of pipeline both conforms to the settlement trough by numerical stimulation and theoretical calculation. For the lining and the grouting pressure being considered, the longitudinal deformation of pipeline of the numerical stimulation is smaller than those of the theoretical calculation.

The deformation of the surrounding soil is induced by these factors, which results in the deformation of pipeline. The longitudinal deformation of the pipeline by theoretical calculation is conservative than those by numerical simulation under the tunnel diameter of 10 m.

4.3 Shielding effect of pipeline

Fig. 14 illustrates the variations of longitudinal deformation of surface soil above excavation with and without pipeline with the distance from the centerline of the tunnel under the excavation. The surface soil above excavation experiences the maximum deformation, 9.88 mm without pipeline and 2.88 mm with pipeline, respectively. The deformation curve of the surface soil above excavation without pipeline is in type of "V", while that with pipeline is the type of "U" curve. Compared with the excavation without pipeline, the deformation of surface soil above pipeline decreases by 70.9 %. This indicates that the pipeline above the excavation has a significant shielding effect on the deformation of surface soil above pipeline. Due to the difference in stiffness between the existing pipeline and soil, the deformation of the pipeline is smaller than that of the soil above the pipeline, resulting in a reduction in deformation of the soil above the pipeline.

5. Conclusions

In this study, theoretical calculation and numerical simulation were carried out to investigate the effect of shield tunneling to the longitudinal deformation of the upper existing pipeline. The in-site monitoring data were used to examine the theoretical calculation. The influence of the soil Poisson's ratio, the tunnel diameter and the shielding effect of pipeline were studied. The conclusions are as follows.

(1) The theoretical derivation for the deformation of the existing pipeline under the tunnel is completed in this study. The existing pipeline is simplified as a Timoshenko beam resting on a Winkler foundation, which considers the shearing effect of the pipeline.

(2) The pipeline and the surface soil above the centerline of the tunnel both experience the maximum deformation. The longitudinal deformation curves of the pipeline and the surface soil conform to the Gaussian curve.

(3) The deformation of the existing pipeline is greatly affected within ± 8m of the centerline of the tunnel during the excavation. The deformation of the pipeline increases significantly when the tunnel underpasses the pipeline.

(4) The pipeline experiences an uplift at ± 20 m of the centerline of the tunnel. The uplift gradually increases as the

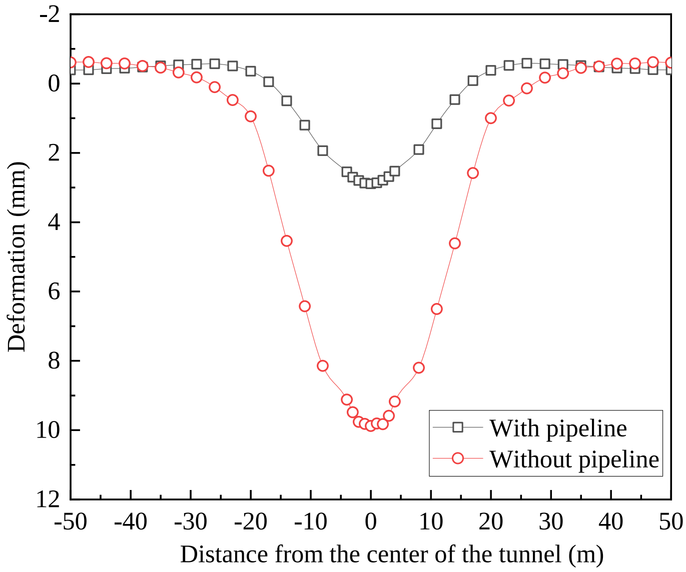

Fig. 14 Variations of surface deformation with distance from the center of the tunnel under with and without pipeline

tunnel excavating. The width of settlement trough is approximately 35 m. The main deformation zone of pipeline affected by the tunnel excavation is within 7 m at both sides of tunnel.

(5) From the parametric study, the Poisson's ratio has a small impact on the deformation of the existing pipeline and surface soil, while the diameter of tunnel has a significant impact on it. The longitudinal deformation of the pipeline by theoretical calculation is conservative than those by numerical simulation under the diameter of the tunnel.

(6) The deformation of surface soil above pipeline decreases by 70.9% compared to the excavation without pipeline. The existence of pipeline has a shielding effect on the deformation of surface soil above the pipeline.

The soil is simplified as a single sandy soil layer in theoretical analysis and numerical simulation. However, the situation of the excavated soil during tunnel construction is complex and multiplex. The author plan to further study the effect of shield tunnel underpass construction under different soil layers on the upper existing pipeline. The results from this study will be compared with the further research.

Acknowledgements

The work presented in this paper was funded by the National Natural Science Foundation of China (Grant No. 52378381).

References

Attewell, P.B., Yeates, J. and Selby, A.R. (1986), *Soil movement induced by tunneling and their effects on pipelines and structures*, Blackie and Son Ltd, London, U.K.

Chen, L.A., Pei, W.W., Yang, Y.H. and Guo, W.L. (2022), "Three-dimensional numerical parametric study of shape effects on multiple tunnel interactions", *Geomech. Eng.*, **31**(3), 237-248. https://doi.org/10.12989/gae.2022.31.3.237.

Chen, W.C., Tang, L.X., Zhao, H.J., Yin, Q., Dong, S., Liu, J., Zhu, Z.H. and Ni, X.D. (2023), "Investigation of three-dimensional deformation mechanisms of existing tunnels due to nearby basement excavation in soft clay", *Geomecha. Eng.*, **34**(2), 115-124. https://doi.org/10.12989/gae.2023.34.2.115.

Ding, Z., Zhang, M.B., Zhang, X. and Wei, X.J. (2023), "Theoretical analysis on the deformation of existing tunnel caused by under-crossing of large-diameter slurry shield considering construction factors", *Tunn. Undergr. Sp. Tech.*, 133. https://doi.org/10.1016/j.tust.2022.104913.

Huang, M.S., Zhou, X.C., Yu, J., Leung, C.F. and Tan, J.Q.W. (2019), "Estimating the effects of tunnelling on existing jointed pipelines based on Winkler model", *Tunn. Undergr. Sp. Tech.*, **86**, 89-99. https://doi.org/10.1016/j.tust.2019.01.015.

Huang, X., Schweiger, H.F. and Huang, H.W. (2013), "Influence of deep excavations on nearby existing tunnels", *Int. J Geomech.*, **13**(2), 170-180. https://doi.org/10.1061/(asce)gm.1943-5622.0000188.

Klar, A., Marshall, A.M., Soga, K. and Mair, R.J. (2008), "Tunneling effects on jointed pipelines", *Can. Geotech. J.*, **45**(1), 131-139. https://doi.org/10.1139/t07-068.

Klar, A., Vorster, T.E.B., Soga, K. and Mair, R.J. (2005), "Soil-pipe interaction due to tunnelling: comparison between Winkler and elastic continuum solutions", *Geotechnique*, **55**(6), 461-466. https://doi.org/10.1680/geot.2005.55.6.461.

Klar, A., Vorster, T.E.B., Soga, K. and Mair, R.J. (2007), "Elastoplastic solution for soil-pipe-tunnel interaction", *J. Geotech. Geoenviron. Eng.*, **133**(7), 782-792. https://doi.org/10.1061/(asce)1090-0241(2007)133:7(782).

Lee, K.M., Rowe, R.K. and Lo, K.Y. (1992), "Subsidence owing to tunnelling. I. Estimating the gap parameter", *Can. Geotech. J.*, **29**(6), 929-940. https://doi.org/10.1016/0148-9062(93)92661-9.

Liang, R.Z., Wu, W.B., Yu, F., Jiang, G.S. and Liu, J.W. (2018), "Simplified method for evaluating shield tunnel deformation due to adjacent excavation", *Tunn. Undergr. Sp. Tech.*, **71**, 94-105. https://doi.org/10.1016/j.tust.2017.08.010.

Liang, R.Z., Xia, T.D., Hong, Y. and Yu, F. (2016), "Effects of above-crossing tunnelling on the existing shield tunnels", *Tunn. Undergr. Sp. Tech.*, **58**, 159-176. https://doi.org/10.1016/j.tust.2016.05.002.

Liang, R.Z., Xia, T.D., Huang, M.S. and Lin, C.G. (2017), "Simplified analytical method for evaluating the effects of adjacent excavation on shield tunnel considering the shearing effect", *Comput. Geotech.*, **81**, 167-187. https://doi.org/10.1016/j.compgeo.2016.08.017.

Lin, C.G., Huang, M.S., Nadim, F. and Liu, Z.Q. (2020), "Tunnelling-induced response of buried pipelines and their effects on ground settlements", *Tunn. Undergr. Sp. Tech.*, **96**, 17. https://doi.org/10.1016/j.tust.2019.103193.

Lin, C.G., Huang, M.S., Nadim, F., Liu, Z.Q. and Yu, J. (2021), "Analytical solutions for tunnelling-induced response of two overlying pipelines", *Tunn. Undergr. Sp. Tech.*, **108**, 14. https://doi.org/10.1016/j.tust.2020.103678.

Lin, X.T., Chen, R.P., Wu, H.N. and Cheng, H.Z. (2019), "Deformation behaviors of existing tunnels caused by shield tunneling undercrossing with oblique angle", *Tunn. Undergr. Sp. Tech.*, **89**, 78-90. https://doi.org/10.1016/j.tust.2019.03.021.

Liu, J.W., Shi, C.H., Lei, M.F., Cao, C.Y. and Lin, Y.X. (2020), "Improved analytical method for evaluating the responses of a shield tunnel to adjacent excavations and its application", *Tunn. Undergr. Sp. Tech.*, **98**, 12. https://doi.org/10.1016/j.tust.2020.103339.

Liu, X., Jiang, A.N., Fang, Q., Wan, Y.S., Li, J.Y. and Guo, X.P. (2022), "Spatiotemporal deformation of existing pipeline due to new shield tunnelling parallel beneath considering construction process", *Appl. Sci.-Basel*, **12**(1), 20. https://doi.org/10.3390/app12010500.

Loganathan, N. and Poulos, H.G. (1998), "Analytical prediction for tunneling-induced ground movements in clays", *J. Geotech. Geoenviron. Eng.*, **124**(9), 846-856. https://doi.org/doi:10.1061/(ASCE)10900241(1998)124:9(846).

Luo, X.P., Lu, S.L., Shi, J.F., Li, X. and Zheng, J.Y. (2015), "Numerical simulation of strength failure of buried polyethylene pipe under foundation settlement", *Eng. Fail. Anal.*, **48**, 144-152. https://doi.org/10.1016/j.engfailanal.2014.11.014.

Marshall, A.M., Klar, A. and Mair, R.J. (2010), "Tunneling beneath buried pipes: View of soil strain and its effect on pipeline behavior", *J. Geotech. Geoenviron. Eng.*, **136**(12), 1664-1672. https://doi.org/10.1061/(asce)gt.1943-5606.0000390.

Nawel, B. and Salah, M. (2015), "Numerical modeling of two parallel tunnels interaction using three-dimensional Finite Elements Method", *Geomech. Eng.*, **9**(6), 775-791. https://doi.org/10.12989/gae.2015.9.6.775.

Shi, J.W., Wang, J.P., Ji, X.J., Liu, H.Q. and Lu, H. (2022), "Three-dimensional numerical parametric study of tunneling effects on existing pipelines", *Geomech. Eng.*, **30**(4), 383-392. https://doi.org/10.12989/gae.2022.30.4.383.

Shi, J.W., Wang, Y. and Ng, C.W.W. (2013), "Buried pipeline responses to ground displacements induced by adjacent static pipe bursting", *Can. Geotech. J.*, **50**(5), 481-492. https://doi.org/10.1139/cgj-2012-0304.

Timoshenko, S.P. (1921), "On the correction for shear of the differential equation for transverse vibrations of prismatic bars", *The London, Edinburgh, and Dublin Philosophical Magazine and J. Science*, **41**(245), 744-746. https://doi.org/10.1080/14786442108636264.

Timoshenko, S.P. (1922), "On the transverse vibrations of bars of uniform cross-section", *The London, Edinburgh, and Dublin Philosophical Magazine and J. Science*, **43**(253), 125-131. https://doi.org/10.1080/14786442208633855.

Vorster, T.E.B., Klar, A., Soga, K. and Mair, R.J. (2005), "Estimating the effects of tunneling on existing pipelines", *J. Geotech. Geoenviron. Eng.*, **131**(11), 1399-1410. https://doi.org/10.1061/(asce)1090-0241(2005)131:11(1399).

Wang, J.X., Cao, A.S., Wu, Z., Sun, Z.P., Lin, X., Sun, L., Liu, X.T., Li, H.B.Q. and Sun, Y.W. (2022), "Numerical simulation on the response of adjacent underground pipelines to super shallow buried large span double-arch tunnel excavation", *Appl. Sci.-Basel*, **12**(2), 24. https://doi.org/10.3390/app12020621.

Wang, Y., Shi, J.W. and Ng, C.W.W. (2011), "Numerical modeling of tunneling effect on buried pipelines", *Can. Geotech. J.*, **48**(7), 1125-1137. https://doi.org/10.1139/t11-024.

Wu, H.N., Shen, S.L., Yang, J. and Zhou, A.N. (2018), "Soil-tunnel interaction modelling for shield tunnels considering shearing dislocation in longitudinal joints", *Tunn. Undergr. Sp. Tech.*, **78**, 168-177. https://doi.org/10.1016/j.tust.2018.04.009.

Wu, W.Y. (2008), *Study on mechanical behaviors of buried pipelines induced by shield tunneling construction*, Hangzhou, Zhejiang University, China [in Chinese].

Yoo, C. and Cui, S.S. (2020), "Effect of new tunnel construction on structural performance of existing tunnel lining", *Geomech. Eng.*, **22**(6), 497-507. https://doi.org/10.12989/gae.2020.22.6.497.

Zhang, S.L., Bao, T. and Liu, C. (2023), "Model tests and numerical modeling of the failure behavior of composite strata caused by tunneling under pipeline leakage conditions", *Eng. Fail. Anal.*, **149**, 13. https://doi.org/10.1016/j.engfailanal.2023.107287.

Zhang, X., Luo, B., Xu, Y.J. and Yang, Z.W. (2024), "Theoretical analysis of stratum horizontal displacements caused by small radius curve shield tunneling", *Comput. Geotech.*, **165**. https://doi.org/10.1016/j.compgeo.2023.105950.

Zhang, Z.G., Zhang, M.X. and Zhao, Q.H. (2015), "A simplified analysis for deformation behavior of buried pipelines considering disturbance effects of underground excavation in soft clays", *Arabian J. Geosci.*, **8**(10), 7771-7785. https://doi.org/10.1007/s12517-014-1773-4.

Zhang, Z.G., Zhao, Q.H. and Zhang, M.X. (2016), "Deformation analyses during subway shield excavation considering stiffness influences of underground structures", *Geomech. Eng.*, **11**(1), 117-139. https://doi.org/10.12989/gae.2016.11.1.117.

GC

Appendix A

Full expressions of some of the matrices and vectors mentioned in the main text are presented below.

$$[K_1]=\frac{EI}{kD_\mathrm{p}l^4}\begin{bmatrix}1 & -4 & 6 & -4 & 1 & & & & \\ & 1 & -4 & 6 & -4 & 1 & & & \\ & & \ddots & \ddots & \ddots & \ddots & \ddots & & \\ & & & 1 & -4 & 6 & -4 & 1 & \\ & & & & 1 & -4 & 6 & -4 & 1\end{bmatrix}_{(\mathrm{n}+1)\times(\mathrm{n}+5)} \quad (13)$$

$$[K_2]=\frac{EI}{GAl^2}\begin{bmatrix}0 & 1 & -2 & 1 & 0 & & & & & \\ & 0 & 1 & -2 & 1 & 0 & & & & \\ & & 0 & 1 & -2 & 1 & 0 & & & \\ & & & \ddots & \ddots & \ddots & \ddots & \ddots & & \\ & & & & 0 & 1 & -2 & 1 & 0 & \\ & & & & & 0 & 1 & -2 & 1 & 0\end{bmatrix}_{(\mathrm{n}+1)\times(\mathrm{n}+5)} \quad (14)$$

$$[K_3]=\begin{bmatrix}0 & 0 & 1 & & & & \\ & 0 & 0 & 1 & & & \\ & & \ddots & \ddots & \ddots & & \\ & & & 0 & 0 & 1 & \\ & & & & 0 & 0 & 1\end{bmatrix}_{(\mathrm{n}+1)\times(\mathrm{n}+5)} \quad (15)$$

$$\{U_1\}=\{u_{z,0},u_{z,1},u_{z,2},u_{z,3},\cdots,u_{z,\mathrm{n}-3},u_{z,\mathrm{n}-2},u_{z,\mathrm{n}-1},u_{z,\mathrm{n}}\}_{1\times(\mathrm{n}+1)}^{\mathrm{T}} \quad (16)$$

$$\{U_2\}=\frac{EI}{GAl^2}\begin{Bmatrix}u_{z,1}-2u_{z,0}+u_{z,-1}\\ u_{z,2}-2u_{z,1}+u_{z,0}\\ u_{z,3}-2u_{z,2}+u_{z,1}\\ u_{z,4}-2u_{z,3}+u_{z,2}\\ \vdots\\ u_{z,\mathrm{n}-2}-2u_{z,\mathrm{n}-3}+u_{z,\mathrm{n}-4}\\ u_{z,\mathrm{n}-1}-2u_{z,\mathrm{n}-2}+u_{z,\mathrm{n}-3}\\ u_{z,\mathrm{n}}-2u_{z,\mathrm{n}-1}+u_{z,\mathrm{n}-2}\\ u_{z,\mathrm{n}+1}-2u_{z,\mathrm{n}}+u_{z,\mathrm{n}-1}\end{Bmatrix}_{1\times(\mathrm{n}+1)} \quad (17)$$